

Mitochondrial Impairment in Oligodendroglial Cells Induces Cytokine Expression and Signaling

Miriam Scheld¹, Athanassios Fragoulis², Stella Nyamoya^{1,3}, Adib Zendedel¹, Bernd Denecke⁴, Barbara Krauspe⁵, Nico Teske³, Markus Kipp⁶, Cordian Beyer¹, Tim Clarner¹

¹Institute of Neuroanatomy, Faculty of Medicine, RWTH Aachen University, 52074 Aachen, Germany, mscheld@ukaachen.de

²Department of Anatomy and Cell Biology, Faculty of Medicine, RWTH Aachen University, 52074 Aachen, Germany

³Department of Anatomy II, Ludwig-Maximilians-University of Munich, 80336 Munich, Germany

⁴IZKF Genomics Facility, Interdisciplinary Center for Clinical Research, RWTH Aachen University, 52074 Aachen, Germany

⁵Clinic for gynaecology and obstetrics, Faculty of Medicine, RWTH Aachen University, 52074 Aachen, Germany

⁶Institute of Anatomy, University of Rostock, 18057 Rostock, Germany

Abstract

Widespread inflammatory lesions within the central nervous system grey and white matter are major hallmarks of multiple sclerosis. The development of full-blown demyelinating multiple sclerosis lesions might be preceded by preactive lesions which are characterized by focal microglia activation in close spatial relation to apoptotic oligodendrocytes. In this study, we investigated the expression of signaling molecules of oligodendrocytes that might be involved in initial microglia activation during preactive lesion formation. Sodium azide was used to trigger mitochondrial impairment and cellular stress in oligodendroglial cells *in vitro*. Among various chemokines and cytokines, IL6 was identified as a possible oligodendroglial cell-derived signaling molecule in response to cellular stress. Relevance of this finding for lesion development was further explored in the cuprizone model by applying short-term cuprizone feeding (2 – 4 d) on male C57BL/6 mice and subsequent analysis of gene expression, *in situ* hybridization and histology. Additionally, we analyzed the possible signaling of stressed oligodendroglial cells *in vitro* as well as in the cuprizone mouse model. *In vitro*, conditioned medium of stressed oligodendroglial cells triggered the activation of microglia cells. In cuprizone-fed animals, IL6 expression in oligodendrocytes was found in close vicinity of activated microglia cells. Taken together, our data supports the view that stressed oligodendrocytes have the potential to activate microglia cells through a specific cocktail of chemokines and cytokines among IL6. IL6. Further studies will have to identify the temporal activation pattern of these signaling molecules, their cellular sources and impact on neuroinflammation.

Introduction

Stressed oligodendrocytes in close proximity to foamy macrophages and clustered microglia expressing HLA-DR are found widespread within the normal appearing white matter of multiple sclerosis (MS) patients (De

40 Groot, Bergers et al. 2001, Zeis, Probst et al. 2009). These preactive lesions are thought to precede the
41 development of full-blown demyelinating MS lesions (De Groot, Bergers et al. 2001, Wuerfel, Bellmann-Strobl
42 et al. 2004, van der Valk and Amor 2009). Therefore, it seems reasonable to assume that the initial microglia
43 activation and clustering as observed in preactive lesions might be triggered by oligodendrocyte-derived
44 signaling molecules. It has been shown that oligodendrocytes are able to secrete a variety of signaling molecules
45 such as chemokines, cytokines and other regulatory proteins which are known to be involved in the regulation of
46 immunological processes (Cannella and Raine 2004, Balabanov, Strand et al. 2007, Kummer, Broekhuizen et al.
47 2007, Okamura, Lebkowski et al. 2007, Tzartos, Friese et al. 2008, Merabova, Kaminski et al. 2012, Ramesh,
48 Benge et al. 2012, Moyon, Dubessy et al. 2015). For example, IFN γ -treated primary rat oligodendrocytes
49 significantly induced the expression of the chemokines CXCL10, CCL2, CCL3, and CCL5 (Balabanov, Strand
50 et al. 2007). Furthermore, the cytokines IL6 and IL8 and the chemokine CCL2 were significantly induced in the
51 human oligodendrocyte cell line MO3.13 when confronted with *Borrelia burgdorferi*. Exposure to the same
52 bacteria caused the induction of IL8 and CCL2 in a dose-dependent manner in primary human oligodendrocytes
53 (Ramesh, Benge et al. 2012).

54 So far, it is not completely understood which processes trigger oligodendrocyte stress and subsequent expression
55 of signaling molecules. One factor leading to oligodendrocyte stress, impaired mitochondrial functions and
56 increased levels of reactive oxygen species (Wang, Wu et al. 2013) might be the accumulation of mutations
57 within the mitochondrial genome. It is known that the mtDNA is prone to mutations with a mutation rate that is
58 about 10-fold higher than chromosomal DNA (Linnane, Marzuki et al. 1989). In comparison to other cell
59 populations, oligodendrocytes have a reduced capacity to repair their mtDNA, possibly due to particularities in
60 the expression of factors involved in DNA repairing mechanisms (Hollensworth, Shen et al. 2000). With respect
61 to demyelination and oligodendrocyte pathology, both mutations in mitochondrial genes as well as oxidative
62 stress play a role in lesion formation and disease progression in MS and MS-related animal models (Mahad,
63 Lassmann et al. 2008, Mao and Reddy 2010, Su, Bourdette et al. 2013, Draheim, Liessem et al. 2016).

64 As the sentinels and injury sensors of the central nervous system (CNS), microglia can be activated by many
65 kinds of mechanical injury and pathological disturbances within the CNS (Perry, Andersson et al. 1993,
66 Gehrmann, Matsumoto et al. 1995). In MS, the magnitude of myelin loss during demyelinating events positively
67 correlates with the number of activated microglia cells (Clarner, Diederichs et al. 2012). Furthermore,
68 microgliosis can be induced by leukocyte infiltration into the CNS (Scheld, Ruther et al. 2016, Ruther, Scheld et
69 al. 2017). However, the listed factors are rather unlikely to contribute to the activation of microglia cells during
70 the formation of preactive lesions, since the affected brain regions lack any signs of demyelination, leukocyte
71 infiltration, astrogliosis or inciting agents such as viral or bacterial antigens (Gay, Drye et al. 1997, De Groot,
72 Bergers et al. 2001, Barnett and Prineas 2004, Marik, Felts et al. 2007, van der Valk and Amor 2009). A growing
73 body of evidence suggests that stressed oligodendrocytes might be active contributors to MS lesion formation by
74 initiating microglia reactivity. Barnett and Prineas have reported areas with an extensive oligodendrocyte
75 apoptosis and concomitant microgliosis in the absence of infiltrating immune cells in the normal appearing white
76 matter of MS patients, thus indicating that oligodendrocyte loss precedes inflammatory demyelination (Barnett
77 and Prineas 2004).

78 In this study, we use the oligodendroglial cell line OLN93 to screen for oligodendrocyte-derived chemokines and
79 cytokines that are potentially able to activate microglia cells. Subsequent culture experiments with the microglia
80 cell line BV2 show that IL6, which is robustly expressed by stressed oligodendroglial cells, is a constituent of a

81 cocktail of secreted proteins, which are responsible for microglia activation. Finally, IL6 expression was
82 explored in the cuprizone model, which recapitulates distinct but important aspects of early MS lesion formation.

83

84 **Materials and methods**

85 **Cell culture**

86 Cells of the oligodendroglial lineage cell line OLN93 were received from Dr C. Richter-Landsberg (RRID:
87 CVCL_5850; Oldenburg, Germany) and chosen as a model system because of strong similarities to primary
88 oligodendrocytes regarding morphology and gene expression (Richter-Landsberg and Heinrich 1996). BV2 cell
89 line was cultured according to Dr. E. Blasi (RRID: CVCL_0182; Modena, Italy) and chosen as a model system
90 because of its suitability to study molecular mechanisms that control induction and expression of biological
91 activities in microglia (Blasi, Barluzzi et al. 1990). Cell lines were not authenticated prior to experiments. None
92 of the cell lines used in these experiments is listed as a commonly misidentified cell line by the International Cell
93 Line Authentication Committee. OLN93 oligodendroglial cell line and BV2 microglial cell lines were
94 maintained in Dulbecco's Modified Eagle Medium supplemented with 5% (OLN93) and 10% (BV2) heat-
95 inactivated fetal bovine serum, penicillin G (10,000 units/mL), and streptomycin (10,000 µg/mL). For
96 experiments, cells were seeded into 6-well dishes, 10 cm culture dishes or 75 cm² flasks at densities of 3 x 10⁵,
97 5 x 10⁶ and 2.3 x 10⁶ cells per well, respectively. Before treatment, cells were cultivated for 24 h in starving
98 medium (OLN93: SATO with 1% penicillin G/ streptomycin; BV2: DMEM supplemented with 0.5% fetal calf
99 serum and 0.5% penicillin G/ streptomycin). Cells were cultivated in a humidified atmosphere of 5% CO₂ at
100 37 °C.

101

102 **Oligodendroglial cell conditioned medium (OCM)**

103 OLN93 cells were treated with 10 mM sodium azide (SA, Sigma Aldrich) or vehicle (UltraPure Distilled Water;
104 Thermo Fisher Scientific) for 24 h. After washing twice with 1x phosphate buffered saline (PBS), cells were
105 incubated with starving medium for a 24 h secretion period. The medium of each treatment group was pooled,
106 centrifuged and filtered through a 20 µm cell strainer. BV2 microglia were incubated with OCM from SA treated
107 cells (OCM-SA) for 6 h. *Oligodendroglial starving* medium and OCM from vehicle groups (OCM-vehicle)
108 served as control. OCM was additionally used for ELISA analysis. See supplementary figure A for experimental
109 overview.

110

111 **Cell Viability and metabolic activity assay**

112 To investigate the toxic effects of the applied SA concentrations, CytoTox 96® Non-Radioactive Cytotoxicity
113 Assay and CellTiter-Blue® Cell Viability Assay (Promega G1780, G8081) were performed according to the
114 manufacturer's instructions. Brief, cells were seeded into an opaque-walled 96 tissue culture plate and treated
115 with SA and vehicle for 24 h. Treatment of cells with a lysis solution served as a negative control as all cells are
116 dead, medium without cells served as blank. Cells were incubated with CellTiter-Blue reagent until a change of
117 color was observed, fluorescence was measured at 560/590 nm with the Tecan infinite M200 plate reader and
118 processed with i-control 1.10 software. Medium of cells was incubated for 30 min with CytoTox96 reagent and
119 the reaction was stopped with stop solution. Absorbance was measured at 490 nm with Tecan i-control software.
120 Data are given in % of control fluorescence and absorbance values, respectively. No blinding was performed for
121 the evaluation of these data. Experiments were performed with 8 biological and 2 technical replicates.

122 **Enzyme-linked immunosorbent assay**

123 IL6 ELISA was conducted using cell culture supernatants of vehicle and SA-treated OLN93 cells (OCM)
124 according to the manufacturer's protocol (Quantikine ELISA, R&D Systems). Color development of substrate
125 solution (stabilized hydrogen peroxide and stabilized chromogen (tetramethylbenzidine)) was monitored with a
126 Tecan infinite M200 plate reader at 450 nm with a wavelength correction at 540 nm and processed with i-control
127 1.10 software. IL6 protein levels are displayed as absolute values in pg/ml. Experiments were performed with
128 two biological and two technical replicates.

129

130 **Animals and cuprizone intoxication**

131 C57BL/6J male mice (19 ± 2 g) were obtained from Janvier and housed under standard laboratory conditions in
132 the animal facility of the Uniklinik Aachen according to the Federation of European Laboratory Animal Science
133 Association's recommendations. Mice were maintained with food and water *ad libitum* in a 12 h light/dark cycle
134 at controlled temperature and humidity ($23 \pm 2^\circ\text{C}$; $55\% \pm 10\%$ humidity). Experimental procedures, i.e.
135 cuprizone feeding, were approved by the Review Board for the Care of Animal Subjects of the district
136 government (Nordrhein-Westfalen, Germany). At noon, mice received a diet containing 0.25 % cuprizone (bis-
137 cyclohexanone-oxaldihydrazone, Sigma Aldrich; choice of concentration via established protocols) for up to 2 d
138 mixed into a ground standard rodent chow. The control group was fed with standard rodent chow. Animals were
139 allocated to groups applying the following procedure: Animals were distributed across cages (three animals per
140 cage; cage area 435 cm^2) and each group consisted of mice with comparable weight. We used cards numbered
141 from 1 to 2 for the respective experimental group (1 = control, 2 = 2 days cuprizone). The number on the card
142 randomly assigned the cages to the respective group. Re-evaluation of cDNA samples of 1 – 4 d cuprizone-
143 treated mice were performed using previously published work from our research group (Krauspe, Dreher et al.
144 2015). Size of groups for each experiment is given in the appropriate figure legends and an experimental
145 overview is shown in supplementary figure B.

146

147 **Tissue preparation**

148 Mice were anaesthetized with ketamine/xylazine (100 mg/kg and 10 mg/kg; i.p. with $100\ \mu\text{l}/10\text{ g}$ body weight)
149 and transcardially perfused with either PBS or 3.7% formalin in PBS. Brains were removed to isolate RNA of
150 the corpus callosum (CC) for gene expression analysis or whole brains were post-fixed in 3.7% formalin and
151 subsequently embedded into paraffin for immunohistological analysis following established protocols (Clarner,
152 Janssen et al. 2015).

153

154 **Immunohistological staining and fluorescence labeling**

155 For fluorescence and immunohistological analysis, $5\ \mu\text{m}$ thick brain slides were cut with a microtome. Rabbit
156 anti-IL6 (Abcam ab7737), mouse anti-OLIG2 (Millipore MABN50), donkey-anti-rabbit 488 and donkey-anti-
157 mouse 594 were used for fluorescence labeling (Life Technologies A21206, A21203). Signal specificity was
158 validated by incubating slices with the respective secondary antibody without pre-incubation with the first
159 antibody (see supplementary figure C). Furthermore, cross reactivity of secondary antibodies with each other or
160 the false primary antibody was additionally excluded (data not shown). For chromogen double labeling, anti-
161 GFAP (Santa Cruz sc-6170), anti-IBA-1 (Millipore MABN92) and anti-APC (Millipore OP80) antibodies were
162 visualized with a horseradish peroxidase enzyme (Vector Labs) and DAB substrate (Dako); anti-IL6 (Abcam

163 ab6672) was visualized with an alkaline phosphatase (Zytomed Systems) and an AP Blue substrate that emits at
164 680 nm (Vector Laboratories).

165

166 **In situ hybridization**

167 Commercial fluorescence *in situ* hybridization kits (QuantiGene View RNA *in situ* hybridization tissue assay;
168 Affymetrix-Panomics) were used for double labeling of formalin-fixed, paraffin-embedded tissue, following the
169 manufacturer's recommendations. Protease digestion time was adjusted to 20 min. Probes directed against *Olig2*
170 and *Il6* were purchased from Affymetrix (Affymetrix-Panomics). Confocal images were captured using the
171 LSM710 laser-scanning microscope station (Carl Zeiss).

172

173 **Chemokine and cytokine array**

174 RNA isolation was performed with RNeasy Micro Kit (Qiagen 74004). Cells were directly lysed with RLT
175 buffer and homogenized with Precellys homogenizer. Further isolation procedures such as washing and DNA
176 digestion was conducted in MinElute spin columns. RNA concentration was measured with NanoDrop 2000
177 spectrometer. 500 ng RNA was reverse transcribed with RT² First Strand Kit (Qiagen 330404). Genomic DNA
178 was eliminated and RNA reverse transcribed according to the manufacturer's instructions. Cytokine &
179 Chemokine RT² Profiler PCR Array (Qiagen PARN-150ZD) was performed with RT² SYBR Green Mastermix
180 and processed with Bio-Rad CFX connect cycler. PCR cycling program was composed of one 10 min 95°C hot
181 start cycle and 40 cycles of 95°C 15 s and 60°C 1 min to perform fluorescence data collection. Results were
182 analyzed using the Data analysis center from Qiagen ([https://www.qiagen.com/de/shop/genes-and-
183 pathways/data-analysis-center-overview-page](https://www.qiagen.com/de/shop/genes-and-pathways/data-analysis-center-overview-page)). β -Actin, β -2 microglobulin, hypoxanthine
184 phosphoribosyltransferase 1, lactate dehydrogenase A and ribosomal protein large P1 served as reference genes.
185 Furthermore, the array contained one genomic DNA control, three replicate reverse-transcription controls to test
186 reverse-transcription efficiency and three replicate positive PCR controls to test PCR efficiency. Experiments
187 were performed with one biological and one technical replicate.

188

189 **Gene expression analysis**

190 RNA for array validation and microglia gene expression analysis was isolated by using peqGold TriFast (Peqlab)
191 and reverse-transcribed in a 20 μ L reaction volume using a reverse-transcription kit (Thermo Fisher Scientific
192 28025-021). cDNA levels were then analyzed by qPCR using SensiMix SYBR® & Fluorescein Kit (Bioline
193 QT615-05) and Bio-Rad CFX connect cycler. The expression levels were calculated relative to the reference
194 genes coding for glyceraldehyde 3-phosphate dehydrogenase or cyclophilin A using the $\Delta\Delta$ Ct method. Primer
195 sequences are given in table I. No blinding was performed for the evaluation of these data. Experiments were
196 performed with at least 6 biological and 2 technical replicates if not stated otherwise. Furthermore, a gene array
197 (Affymetrix) from the corpus callosum (CC) of control animals and animals that were fed cuprizone for 2 d, was
198 re-evaluated with respect to those genes identified in the OLN93 gene expression study (Krauspe, Dreher et al.
199 2015).

200 Table I. Forward and reverse primer sequences used for qPCR analysis.

Name	Forward sequence 5'-3'	Reverse sequence 5'-3'
Arg1 mouse	CTCCAAGCCAAAGTCCTTAGAG	AGGAGCTGTCATTAGGGACATC
Atf3 rat	ACTGCGTTGTCCCACTCTGT	TCATCTGAGAATGGCCGGGA
Csf1 rat	AGCAAGGAAGCGAACGAAC	ATGTGGCTACAGTGCTCCGA
Cyca rat	GGCAAATGCTGGACCAAACAC	TTAGAGTTGTCCACAGTCGGAGATG
Ddit3 rat	TGTTGAAGATGAGCGGGTGG	GCTTTCAGGTGTGGTGGTGT
Gapdh mouse	TGTGTCCGTCGTGGATCTGA	CCTGCTTCACCACCTTCTTGA
Gdf15 rat	TCAGCTGAGGTTCTGCTGTTC	GCTCGTCCGGGTTGAGTTG
Il6 mouse	GATACCACTCCCAACAGACCTG	GGTACTCCAGAAGACCAGAGGA
Il6 rat	TCTCTCCGCAAGAGACTTCCA	ATACTGGTCTGTTGTGGGTGG
Lif rat	TTTGCCGTCTGTGCAACAAG	TGGACCACCGCACTAATGAC
Nos2 mouse	ACATCGACCCGTCCACAGTAT	CAGAGGGGTAGGCTTGTCTC
Spp1 rat	CCAGCCAAGGACCAACTACA	TCTCCTCTGAGCTGCCAAAC

201

202 Statistical analysis

203 Statistical analysis was performed using JMP10 and GraphPad Prism 5. Data are presented as arithmetic means
 204 \pm SEM. To test for equal variances, Bartlett test was performed. Data transformations via Boxcox for
 205 homoscedasticity are indicated if necessary. Shapiro-Wilk test was used to test for normal distribution.
 206 Parametric data were analyzed with one-way ANOVA followed by Tukey's post hoc test for multiple
 207 comparisons or with Student's t-test. Non-parametric data were analyzed with Kruskal-Wallis test followed by
 208 the Dunn's multiple comparison or Mann-Whitney test. $p < 0.05$ was considered statistically significant. The
 209 following symbols were used to indicate the level of significance: * $p < 0.05$, ** $p < 0.005$, *** $p < 0.001$; ns
 210 indicates not significant. No outliers were excluded from the analyses. No sample size calculation was
 211 performed.

212

213 Results

214 Sodium azide induces stress in oligodendroglial cells

215 SA is a potent inhibitor of the mitochondrial respiratory chain and inhibits the mitochondrial complex IV which
 216 is responsible for the transfer of cytochrome c to an oxygen molecule (Bennett, Mlady et al. 1996, Teske,
 217 Liessem et al. 2018). To induce a breakdown of the mitochondrial inner transmembrane potential (i.e. sub-lethal
 218 mitochondrial stress reaction), the oligodendroglial cell line OLN93 was stimulated with 10 mM sodium azide
 219 (SA) for 24 h as previously described by Teske et al. (Teske, Liessem et al. 2018). Afterwards, cells were kept in
 220 culture for additional 24 h to produce OCM (oligodendroglial cell conditioned medium). To confirm that the
 221 used SA concentration was not inducing immediate cell death, lactate dehydrogenase (LDH) cytotoxicity assay
 222 and cell titer blue viability assay were performed after 24 h of SA-treatment. Results are shown in figure 1A.
 223 LDH levels in the cell culture supernatants were significantly increased after SA treatment compared to vehicle,
 224 indicating cell death; LDH levels of lysis control was significantly increased compared to both treatment groups

225 (left histogram in figure 1A). SA-induced LDH release was paralleled by a trend towards lower levels of
226 metabolic activity in these cells (right histogram in figure 1A) however this difference was not statistically
227 significant. Additionally, 10 mM SA-treated OLN93 cells did not show major morphological changes or loss of
228 cell numbers at the microscopic level (figure 1B). *Ddit3* and *Atf3* are members of the integrated stress response
229 which is closely connected to oxidative stress. Gene expression analysis of *Ddit3* (Rutkowski, Arnold et al.
230 2006, Puthalakath, O'Reilly et al. 2007) and *Atf3* (Edagawa, Kawauchi et al. 2014) was measured after the 24 h
231 secretion phase via qPCR to confirm endoplasmic reticulum stress in SA-treated cells on the transcriptional level
232 (figure 1C).

233

234 **Stressed oligodendroglial cells secrete various cytokines and chemokines**

235 In a next step, we aimed to analyze the gene expression of secreted molecules that oligodendroglial cells produce
236 upon SA-induced mitochondrial stress. To get a first hint about the possible identity of such signaling molecules,
237 we performed PCR arrays that screened for mRNA expression levels of 84 cytokines and chemokines with one
238 sample ($n = 1$). Out of the 84 investigated genes, 13 were induced by at least 2-fold when comparing the SA
239 group with the vehicle group. Those 13 genes are displayed in figure 2A. IL6 and GDF15 were most robustly
240 induced in stressed oligodendroglial cells compared to cells treated with vehicle. To confirm validity of the path
241 finding gene array, we performed qPCR in independent samples from two additional experiments with each
242 $n = 6$ for IL6, GDF15 and 3 randomly assigned genes (figure 2B). As indicated in figure 2B, IL6 gene
243 expression and GDF15 gene expression were found to be induced > 12-fold in qPCR analysis in SA-treated
244 OLN93 cells. Differences in between the gene expression measured in array analysis vs. qPCR are likely due to
245 different evaluation strategies, i.e. different reference genes and subsequent software analysis and the measuring
246 of only one sample in the PCR array. In comparison, genes for SPP1, LIF and CSF1 were induced 2.5- to 4-fold.
247 In a next step, the relevance of the identified factors *in vivo* was investigated. Since short-term cuprizone
248 intoxication mimics early lesion formation and induces stress in oligodendroglial cells, we re-evaluated gene
249 array data from the CC of 2 d cuprizone-fed and control animals (Krauspe, Dreher et al. 2015). Results of this
250 evaluation are shown in figure 2C. Out of the 13 investigated genes, 7 were significantly induced. Although
251 GDF15 and CCL7 were highest induced in the tissue samples from cuprizone fed animals, oligodendroglial cells
252 might be responsible - at least in part - for the increased IL6 expression *in vivo*. In a next step, we investigated
253 whether oligodendroglial cells secrete IL6 on the protein level. Therefore, sandwich ELISA was performed using
254 OCM from SA-treated and vehicle-treated oligodendroglial cells. Results are shown in figure 2E and
255 demonstrate a 4-fold increase in IL6 levels upon SA-treatment. Our data show that stressed oligodendroglial
256 cells express various signaling molecules that potentially activate microglia cells. To further investigate this
257 hypothesis, the activation state of microglia cells was evaluated in OCM-stimulated BV2 microglia.
258 Morphologically, no differences were found between cells growing in control medium (DMEM 0.5 %) and those
259 cells grown in OCM-SA. Representative pictures after 6 hours incubation time are shown in figure 2D.
260 Additionally performed arborization analysis and counting of bipolar cells did not reveal morphological changes
261 in response to OCM-SA (supplementary figure E).

262 Expression levels of typical pro- and anti-inflammatory microglia markers were measured by means of qPCR 6 h
263 after beginning of treatment (see supplementary figure A for experimental overview). Results of these
264 experiments are shown in figure 2F. Gene expression of the anti-inflammatory marker arginase 1 was induced
265 when BV2 microglia cells were treated with OCM from SA-treated oligodendroglial cells compared to OCM-

266 vehicle-treated BV2 microglia. One factor that is known to be induced in microglia cells upon pro-inflammatory
267 stimulation is NOS2 (Kempuraj, Thangavel et al. 2016). OCM-SA-treated BV2 microglia displayed an induced
268 expression of NOS2 compared to control. Blocking of IL6 with anti-IL6 antibody only partly counteracted
269 OCM-SA effects (figure 2G) and none of the used concentrations of IL6 protein (10, 30 and 50 ng/ml) was
270 sufficient to show BV2 microglia responses with respect to the gene expression of both Nos2 and Arg1,
271 indicating that other secreted molecules contribute to microglia activation in this scenario (supplementary figure
272 F).

273

274 **Oligodendrocytes are a source of IL6 in vivo**

275 To investigate whether oligodendrocytes might be a relevant source of signaling molecules *in vivo*, we included
276 short-term cuprizone-intoxicated mice (up to 4 d cuprizone) in the study. Since IL6 was highly induced in
277 oligodendroglial cells *in vitro*, we focused on this molecule in this part of the study. Immunohistochemistry,
278 qPCR and *in situ* hybridization were performed on brain slices of cuprizone-intoxicated animals. After 2 d of
279 cuprizone intoxication, IBA-1 immunohistochemistry revealed that microglia display an activated cell
280 morphology in the CC (i.e. less ramified, swollen somata) compared to control mice (figure 3A). Similar
281 morphological changes as well as an increase in microglia cell numbers in early cuprizone-induced lesions have
282 been published previously by our group after a 2 d exposure to cuprizone (Clarner, Janssen et al. 2015, Krauspe,
283 Dreher et al. 2015). Re-evaluation via qPCR revealed that IL6 gene expression was increased about 5-fold in the
284 CC after 2 d of cuprizone intoxication ((Krauspe, Dreher et al. 2015), figure 3B, $n \geq 3$). This induction further
285 increased up to 17-fold after 4 d of cuprizone intoxication. *In situ* hybridization showed an increase of IL6
286 mRNA signals in the CC of cuprizone-intoxicated animals compared to controls (figure 3C, left panel). Double
287 *in situ* hybridization (figure 3C, right panel) and validation by fluorescence double labeling of Olig2 and IL6
288 proteins (figure 3D) as well as double chromogen labeling of APC and IL6 proteins (figure 3E) revealed
289 oligodendroglial cells as one source of IL6 at this early time point (see supplementary figure B for experimental
290 overview). Although APC as well labels astrocytes and neurons in the brain, the double-positive cell in figure 3E
291 resembles morphologically strongly an oligodendrocyte. Three cuprizone-fed animals were investigated and
292 IL6/Olig2 and APC positive cells were found in the CC in all three animals. Since confocal Z-stack analysis was
293 necessary to undoubtedly identify double-positive cells, no quantification of the number of these cells could be
294 performed. Note that oligodendrocytes are not the sole source of IL6 but also other glial cells such as astrocytes
295 express IL6 after 2 days of cuprizone feeding (see supplementary figure D). Tezuka and colleagues also
296 identified astrocytes as a source of IL6 in this model (Tezuka, Tamura et al. 2013).

297

298 **Discussion**

299 The contribution of stressed oligodendrocytes to the formation of inflammatory CNS lesions is only
300 incompletely understood. Here, we induced oligodendrocyte stress by using the mitochondrial inhibitor SA *in*
301 *vitro* and cuprizone intoxication *in vivo*. *In vitro*, this treatment caused a selective increase in the
302 oligodendroglial expression of a variety of immune-modulatory factors such as IL6, GDF15 and a number of
303 chemokines. The expression of IL6 in the *in vivo* situation was explored by qPCR analysis, ELISA, *in situ*
304 hybridization and immunohistological staining of tissue from short-term cuprizone-intoxicated mice.
305 Fluorescence double labeling and *in situ* hybridization of OLIG2 and IL6 identified oligodendrocytes as possible
306 source of this molecule *in vivo* (Ramesh, Benge et al. 2012). These results indicate that our *in vitro* data obtained

307 from SA-treated oligodendroglial cells might be relevant for the *in vivo* situation. It has to be mentioned at this
308 point, that oligodendrocytes are not the sole source of these molecules *in vivo*. With respect to IL6, astrocytes
309 and microglia have been shown to be additional sources in cuprizone intoxication. We would like to point out
310 that due to the high number of possibly involved molecules and the highly complex interplay of different glia
311 cells in the formation of early inflammatory lesions, knock-out mice deficient for single molecules would be of
312 limited use to further investigate the role of oligodendrocytes in this scenario.

313 Regarding the role of IL6 in CNS inflammation and regeneration in general it has been shown that on one hand,
314 it is neuroprotective via accelerating nerve regeneration following trauma or spinal cord injury (Hirota, Kiyama
315 et al. 1996, Yang, Wen et al. 2012) and protects mice from demyelination in the cuprizone model by inducing a
316 specific activation state in microglia (Petkovic, Campbell et al. 2017). On the other hand, IL6 supports chronic
317 inflammatory processes in disorders such as Alzheimer's disease (Swardfager, Lanctot et al. 2010). In active
318 demyelinating MS lesions, IL6 expression by astrocytes and macrophages is relevant for the preservation of
319 oligodendrocytes (Schonrock, Gawlowski et al. 2000). IL6 signaling and mitochondrial functions are closely
320 linked, since IL6 protects cells against a loss of mitochondrial complex IV after bacterial infection in mice
321 (Maiti, Sharba et al. 2015). In the liver, IL6 is necessary for the repair of mitochondrial mutations caused by
322 ethanol intoxication (Zhang, Tachibana et al. 2010). The physiological IL6 concentration in blood plasma
323 samples from healthy humans is about 1 - 1.5 pg/ml whereas the concentration in inflammatory conditions is
324 highly increased and might reach up to 1,000 pg/ml in severe inflammation (Damas, Ledoux et al. 1992, Seino,
325 Ikeda et al. 1994, Ridker, Rifai et al. 2000). This is comparable to the concentrations we measured in the
326 medium of stressed oligodendroglial cells (app. 800 pg/ml). Regarding the IL6 concentrations within the brain,
327 both in healthy and inflamed tissue, only little is known. Therefore further studies will have to show the local
328 IL6 concentrations and precise source within brain tissue in distinct pathologies. With respect to microglia cells,
329 it has been shown that a concentration of 100 ng/ml does activate Nos2 mRNA expression in BV2 microglia
330 (Matsumoto, Dohgu et al. 2018). Furthermore, IL6 (50 ng/ml) increases the mitochondrial Ca²⁺ levels in a
331 STAT3-dependent manner in CD4⁺ T cells (Yang, Lirussi et al. 2015). By using Luciferin-expressing mice, we
332 recently demonstrated that cuprizone intoxication causes an early induction of Nrf2-ARE signaling within the
333 brain (Draheim, Liessem et al. 2016). Since Nrf2 has been shown to regulate IL6 expression (Wruck, Streetz et
334 al. 2011), the increase in oxidative stress and subsequent Nrf2-activation might be a possible mechanism by
335 which IL6 expression is initially triggered in oligodendrocytes in this model. Further studies including Nrf2-
336 deficient mice will have to show the link between oxidative stress and Nrf2 activity on one hand and the
337 expression of IL6 in oligodendrocytes on the other hand. Given this data, we consider this early IL6 expression
338 by oligodendrocytes during preactive lesion formation as a potential first "call for help" by metabolically
339 dysfunctional or oxidatively challenged oligodendrocytes.

340 Another member of the IL6 cytokine family that was induced upon SA-stimulation in this study is LIF, which
341 similar to IL6 signals through the JAK/STAT pathway. It is required for the induction of inflammatory responses
342 of microglia and astrocytes to brain damage (Holmberg and Patterson 2006). Furthermore, it has been shown that
343 LIF plays a role in the initial infiltration of inflammatory cells into the CNS and in the neuronal response to brain
344 injury (Sugiura, Lahav et al. 2000). Another highly induced molecule in our study was GDF15, also known as
345 macrophage inhibitory cytokine-1. Bonaterra et al. showed that GDF15 is functionally linked to IL6 signaling
346 since it regulates inflammatory IL6-dependent processes in vascular injury (Bonaterra, Zugel et al. 2012). A
347 study on the tumorigenesis of prostate carcinoma indicated that the expression of GDF15 is upregulated by IL6

348 (Tsui, Chang et al. 2012). Despite these links to IL6 signaling, GDF15 plays a major role in regulating
349 inflammatory pathways in injured tissues and is involved in pathological processes such as cancer,
350 cardiovascular disorders, ischemia and atherosclerosis (Schlittenhardt, Schmiedt et al. 2005, Kempf, Eden et al.
351 2006, Jiang, Wen et al. 2016).

352 A number of chemokines were induced in SA-treated OLN93 cells that are known to be involved in microglia
353 activation, including CXCL1 and CCL5 (Škuljec, Sun et al. 2011). The cytokine-like glycoprotein SPP1, also
354 known as osteopontin, was induced about 4-fold in stressed oligodendroglial cells. Osteopontin has been
355 implicated in the pathogenesis of several autoimmune diseases such as rheumatoid arthritis, autoimmune
356 hepatitis and MS (Chabas, Baranzini et al. 2001, Yumoto, Ishijima et al. 2002, Mochida, Yoshimoto et al. 2004).
357 Furthermore, osteopontin activity is found in MS lesions (Chen, Chen et al. 2009). It has been shown that the
358 treatment of mixed cortical cultures with osteopontin leads to a stimulation of myelin basic protein expression
359 and the formation of myelin sheaths indicating a putative role in remyelination and recovery (Selvaraju,
360 Bernasconi et al. 2004). CSF1, a macrophage colony-stimulating factor was induced 2.5-fold in SA-stressed
361 oligodendroglial cells and is involved in the proliferation, differentiation, and chemotactic activity of monocytes
362 and macrophages. Interestingly, the survival of adult murine microglia cells seems to be fully dependent upon
363 CSF1 receptor signaling, since all microglia cells can be eliminated from the CNS through CSF1R inhibitor
364 administration (Elmore, Najafi et al. 2014).

365 All of the above mentioned signaling molecules might account - either alone or in combination - for the effects,
366 we observed in OCM-treated microglia cells. Our data indicate that not a sole oligodendroglial cell-derived
367 molecule but rather a combination of different factors account for the activation of microglia cells.

368 In summary, our data supports the view that stressed oligodendrocytes have the potential to activate microglia
369 cells through a specific cocktail of chemokines and cytokines such as IL6. Further studies will have to identify
370 the temporal activation pattern of these signaling molecules, their cellular sources and impact on
371 neuroinflammation.

372

373 **Acknowledgements**

374 The excellent support by Helga Helten, Petra Ibold and Uta Zahn is appreciated. We thank Prof. Dr.
375 Reinhard Windoffer and Dr. Volker Buck for their assistance with confocal microscopy and PD Dr. Claudia
376 Krusche for technical support.

377

378 **Funding Information**

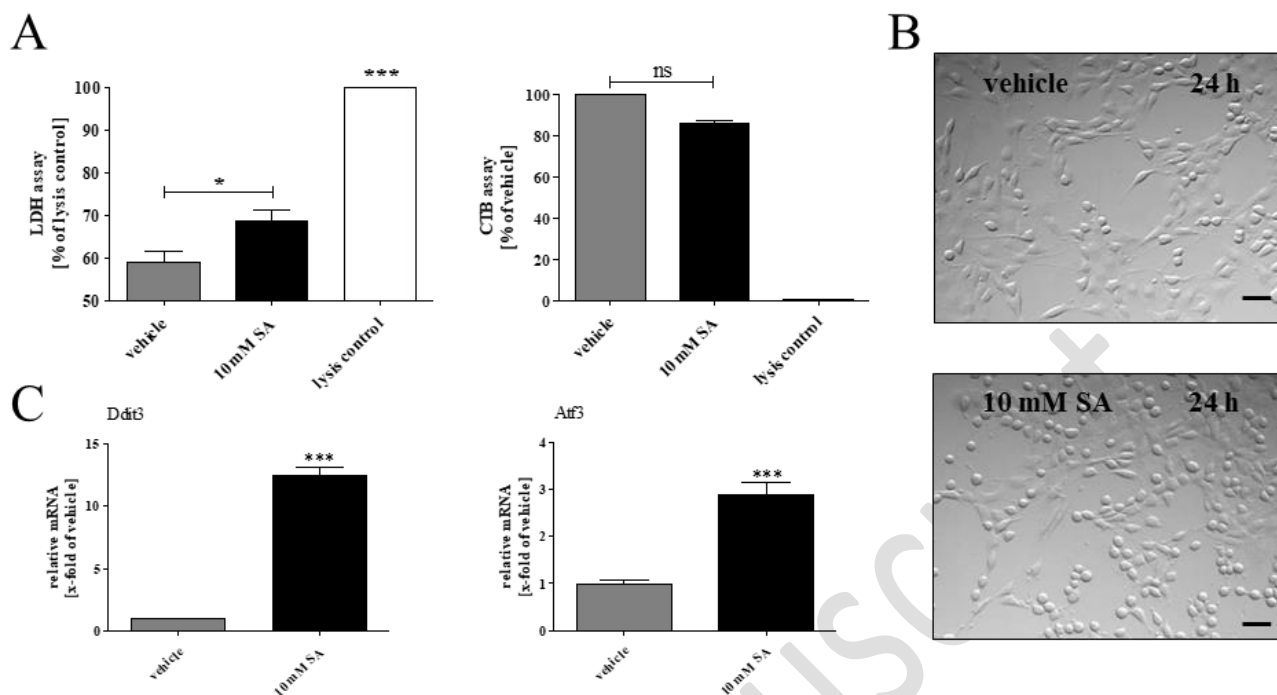
379 Grant sponsor: This study was funded by the START program of the medical faculty of the RWTH Aachen
380 University (M.S.).

381

382 **Compliance with ethical standards**

383 **Conflict of Interest**

384 The authors declare that they have no conflict of interest.



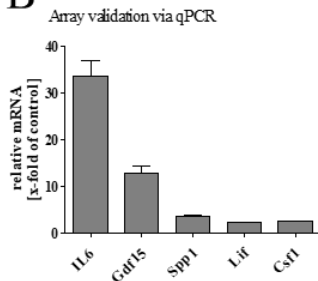
386 Figure 1

387 (A) Shows the cytotoxicity (left) assay normalized to the lysis control and cell viability (right) assay normalized
 388 to the vehicle-treated cells of SA- and vehicle-treated OLN93 cells (eight culture wells, one experiment). (B)
 389 Microscopic pictures using the FLoid™ Cell Imaging station (Thermo Fisher Scientific) of vehicle and SA-
 390 treated oligodendroglial cells did not reveal obvious signs of cell loss or death (20X magnification). (C) Gene
 391 expression analysis of Ddit3 and Atf3 (BoxCox-Y transformed) in vehicle- and SA-treated oligodendroglial cells
 392 indicating metabolic stress (at least six culture wells, five independent experiments). ns = not significant,
 393 * $p < 0.05$, ** $p < 0.005$, *** $p < 0.001$, vehicle = up H₂O, scale bars 50 μ m

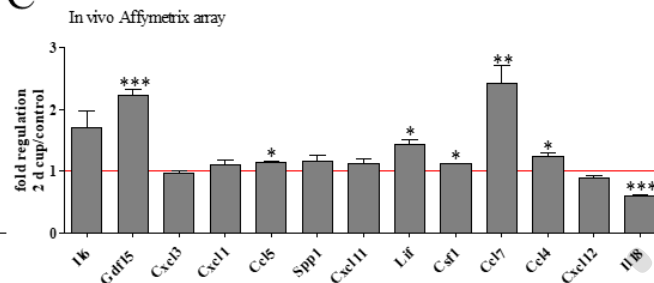
A

Gene Symbol	Il6	Gdf15	Cxcl3	Cxcl1	Ccl5	Spp1	Cxcl11	Lif	Csf1	Ccl7	Ccl4	Cxcl12	Il18
Fold regulation	40.50	34.99	9.88	4.44	4.41	3.80	3.71	2.73	2.52	2.32	2.23	2.17	2.05

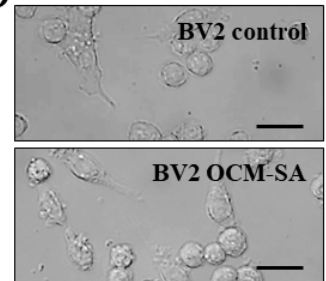
B



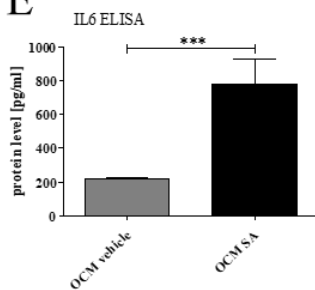
C



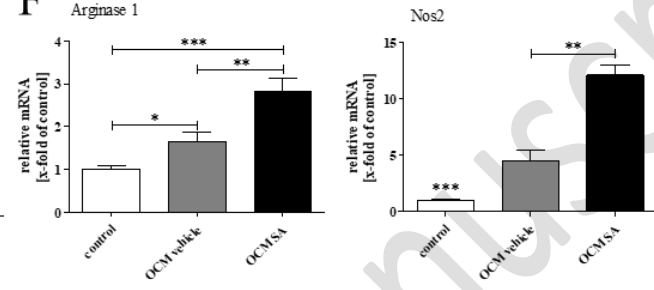
D



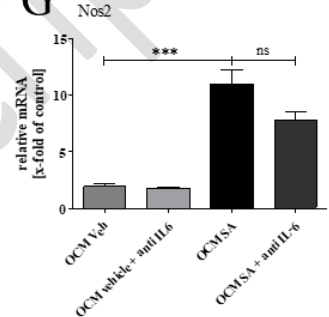
E



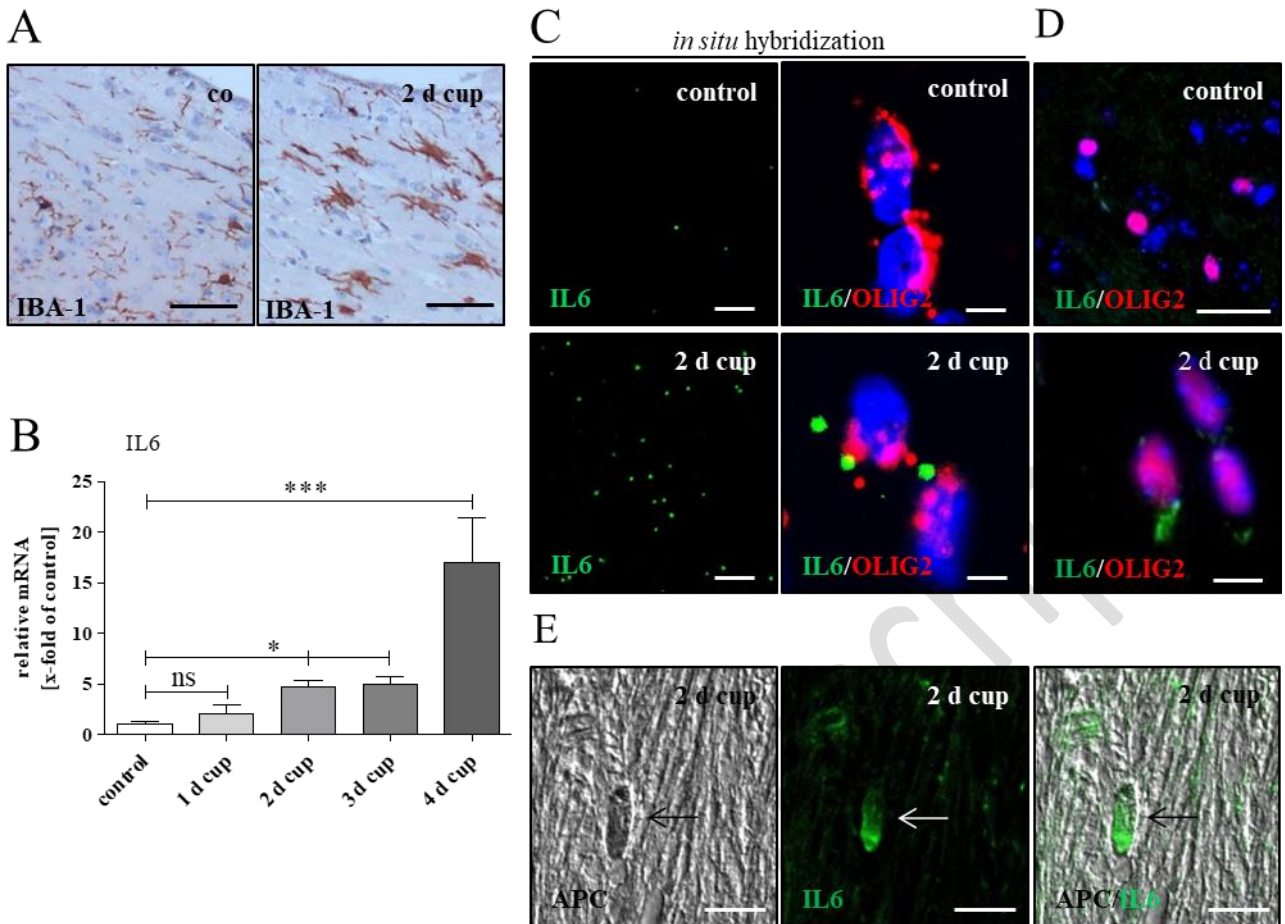
F



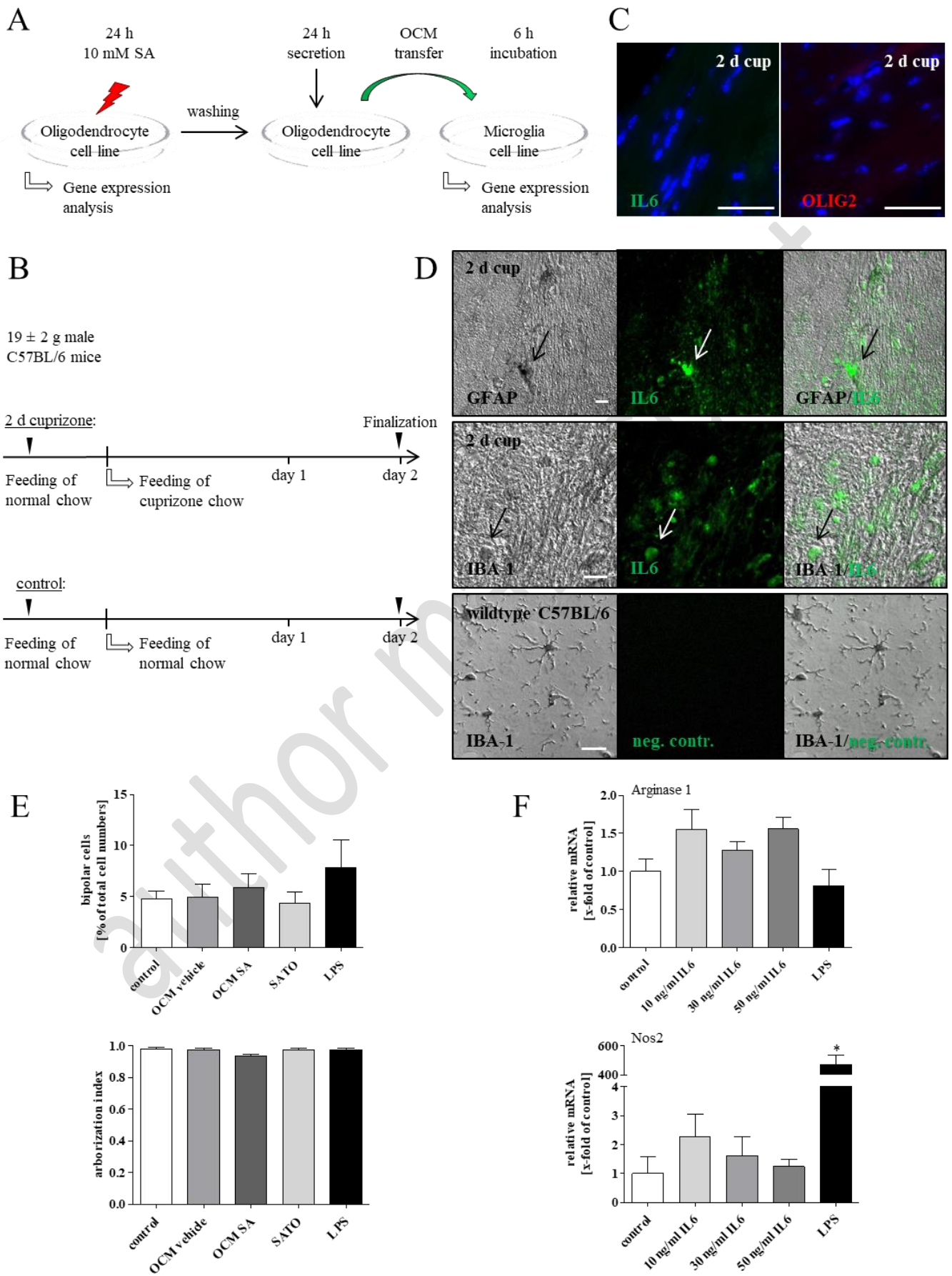
G



394 Figure 2
 395 (A) Shows the fold difference of all chemokines and cytokines that were induced at least 2-fold in SA-treated
 396 OLN93 cells compared to control in the PCR array. (B) To validate the PCR array results, the gene expression
 397 was analyzed via qPCR on independent samples (at least six culture wells, two independent experiments). In (C)
 398 the re-evaluation of a gene array from the CC of 2d cuprizone-intoxicated mice is shown. Data are displayed as
 399 fold induction of control. Note that a selective induction of the identified factors in oligodendroglial cells might
 400 be obscured due to the fact that this array measured expression in the whole tissue and not exclusively in
 401 oligodendrocytes (three animals per group, one experiment, see Krauspe, Dreher et al. 2015). (D) Shows
 402 representative pictures after 6 hours incubation time of BV2 microglia cells with OCM-SA and DMEM 0.5 %
 403 (control). (E) IL6 protein levels increased up to 4-fold in stressed oligodendroglial cells versus unstressed
 404 oligodendroglial cells (BoxCox-Y transformed; six samples each group, two independent experiments). (F)
 405 Shows the gene expression results of pro- and anti-inflammatory markers arginase 1 (BoxCox-Y transformed)
 406 and Nos2 of OCM-stimulated microglia cells (at least five culture wells, four independent experiments). (G)
 407 Induction of Nos2 expression by OCM was partly (not significant) counteracted by anti-IL6 antibody in the
 408 media. ns = not significant, *p < 0.05, **p < 0.005, ***p < 0.001, vehicle = up H₂O, scale bars 30 μm



409 Figure 3
 410 (A) IBA-1⁺ microglia cells display an activated morphology upon short-term cuprizone intoxication compared to
 411 control mice (scale bars 50 μ m). (B) IL6 gene expression was increased in the CC after 2, 3, and 4 d of
 412 cuprizone intoxication compared to untreated animals (re-evaluation of cDNA of short-term cuprizone-fed mice;
 413 BoxCox-Y transformed). (C) At 2 d of 0.25% cuprizone intoxication, the signal for IL6 mRNA was increased
 414 compared to the control. *In situ* hybridization of OLIG2 and IL6 identified oligodendrocytes as source of IL6
 415 production after short-term cuprizone intoxication (scale bars for IL6 20 μ m, for IL6/OLIG2 5 μ m), which was
 416 further validated via fluorescence double labeling of OLIG2 and IL6 (scale bars for control 25 μ m, for 2 d cup
 417 10 μ m) (D) and double labeling of IL6 and APC (scale bars 10 μ m) (E) (three animals per group, one experiment
 418 for figure A – D). ns = not significant, * p < 0.05, ** p < 0.005, *** p < 0.001



420 (A) Schematic illustration of the *in vitro* experimental setup for oligodendroglial cell stimulation and subsequent
421 microglia stimulation with OCM. Oligodendroglial cells (OLN93) were stressed with 10 mM SA for 24 h,
422 medium changed and incubated for 24 h with or without SA to produce OCM-vehicle and OCM-SA,
423 respectively. OCM was then used to stimulate microglia cells for 6 h. (B) Time-line diagram of the 2 d cuprizone
424 feeding *in vivo* experiments. (C) Signal specificity was validated by incubating slices with the respective
425 secondary antibody without pre-incubation with the first antibody. Results for IL6 and OLIG2 negative controls
426 are shown. Note that no signal was found within the examined tissue regions for any secondary antibody (scale
427 bars 50 μm). Cross reactivity of secondary antibodies with each other or the false primary antibody was
428 additionally excluded (data not shown). (D) Double labeling of IL6 with GFAP and IBA-1 (scale bars 10 μm)
429 shows that also other glial cells than oligodendrocytes are possible sources of IL6 in 2 d cuprizone intoxication.
430 No signal was found in the wildtype negative control (lower row) (scale bars 20 μm). (E) No morphological
431 changes such as an increase in the number of bipolar cells or an increased arborization were found in OCM-SA-
432 stimulated compared to OCM-Veh-stimulated BV2 microglia cells. (F) Shows the gene expression results of
433 arginase 1 and Nos2 (BoxCox-Y transformed) of IL6-stimulated microglia cells (four culture wells, one
434 experiment). LPS stimulation served as a positive control for Nos2 induction. * $p < 0.05$, vehicle = up H₂O

435 **References**

- 436 Balabanov, R., K. Strand, R. Goswami, E. McMahon, W. Begolka, S. D. Miller and B. Popko (2007).
437 "Interferon-gamma-oligodendrocyte interactions in the regulation of experimental autoimmune
438 encephalomyelitis." J Neurosci **27**(8): 2013-2024.
- 439 Barnett, M. H. and J. W. Prineas (2004). "Relapsing and remitting multiple sclerosis: pathology of the newly
440 forming lesion." Ann Neurol **55**(4): 458-468.
- 441 Bennett, M. C., G. W. Mlady, Y. H. Kwon and G. M. Rose (1996). "Chronic in vivo sodium azide infusion
442 induces selective and stable inhibition of cytochrome c oxidase." J Neurochem **66**(6): 2606-2611.
- 443 Blasi, E., R. Barluzzi, V. Bocchini, R. Mazzolla and F. Bistoni (1990). "Immortalization of murine microglial
444 cells by a v-raf/v-myc carrying retrovirus." J Neuroimmunol **27**(2-3): 229-237.
- 445 Bonaterra, G. A., S. Zugel, J. Thogersen, S. A. Walter, U. Haberkorn, J. Strelau and R. Kinscherf (2012).
446 "Growth differentiation factor-15 deficiency inhibits atherosclerosis progression by regulating interleukin-6-
447 dependent inflammatory response to vascular injury." J Am Heart Assoc **1**(6): e002550.
- 448 Cannella, B. and C. S. Raine (2004). "Multiple sclerosis: cytokine receptors on oligodendrocytes predict innate
449 regulation." Ann Neurol **55**(1): 46-57.
- 450 Chabas, D., S. E. Baranzini, D. Mitchell, C. C. Bernard, S. R. Rittling, D. T. Denhardt, R. A. Sobel, C. Lock, M.
451 Karpuj, R. Pedotti, R. Heller, J. R. Oksenberg and L. Steinman (2001). "The influence of the proinflammatory
452 cytokine, osteopontin, on autoimmune demyelinating disease." Science **294**(5547): 1731-1735.
- 453 Chen, M., G. Chen, H. Nie, X. Zhang, X. Niu, Y. C. Zang, S. M. Skinner, J. Z. Zhang, J. M. Killian and J. Hong
454 (2009). "Regulatory effects of IFN-beta on production of osteopontin and IL-17 by CD4+ T Cells in MS." Eur J
455 Immunol **39**(9): 2525-2536.
- 456 Clarner, T., F. Diederichs, K. Berger, B. Denecke, L. Gan, P. van der Valk, C. Beyer, S. Amor and M. Kipp
457 (2012). "Myelin debris regulates inflammatory responses in an experimental demyelination animal model and
458 multiple sclerosis lesions." Glia **60**(10): 1468-1480.
- 459 Clarner, T., K. Janssen, L. Nellessen, M. Stangel, T. Skripuletz, B. Krauspe, F. M. Hess, B. Denecke, C.
460 Beutner, B. Linnartz-Gerlach, H. Neumann, L. Vallieres, S. Amor, K. Ohl, K. Tenbrock, C. Beyer and M. Kipp
461 (2015). "CXCL10 triggers early microglial activation in the cuprizone model." J Immunol **194**(7): 3400-3413.
- 462 Damas, P., D. Ledoux, M. Nys, Y. Vrindts, D. De Groote, P. Franchimont and M. Lamy (1992). "Cytokine
463 serum level during severe sepsis in human IL-6 as a marker of severity." Ann Surg **215**(4): 356-362.
- 464 De Groot, C. J., E. Bergers, W. Kamphorst, R. Ravid, C. H. Polman, F. Barkhof and P. van der Valk (2001).
465 "Post-mortem MRI-guided sampling of multiple sclerosis brain lesions: increased yield of active demyelinating
466 and (p)reactive lesions." Brain **124**(Pt 8): 1635-1645.
- 467 Draheim, T., A. Liessem, M. Scheld, F. Wilms, M. Weissflog, B. Denecke, T. W. Kensler, A. Zendedel, C.
468 Beyer, M. Kipp, C. J. Wruck, A. Fragoulis and T. Clarner (2016). "Activation of the astrocytic Nrf2/ARE system
469 ameliorates the formation of demyelinating lesions in a multiple sclerosis animal model." Glia **64**(12): 2219-
470 2230.
- 471 Edagawa, M., J. Kawauchi, M. Hirata, H. Goshima, M. Inoue, T. Okamoto, A. Murakami, Y. Maehara and S.
472 Kitajima (2014). "Role of activating transcription factor 3 (ATF3) in endoplasmic reticulum (ER) stress-induced
473 sensitization of p53-deficient human colon cancer cells to tumor necrosis factor (TNF)-related apoptosis-
474 inducing ligand (TRAIL)-mediated apoptosis through up-regulation of death receptor 5 (DR5) by zerumbone and
475 celecoxib." J Biol Chem **289**(31): 21544-21561.

476 Elmore, M. R., A. R. Najafi, M. A. Koike, N. N. Dagher, E. E. Spangenberg, R. A. Rice, M. Kitazawa, B.
477 Matusow, H. Nguyen, B. L. West and K. N. Green (2014). "Colony-stimulating factor 1 receptor signaling is
478 necessary for microglia viability, unmasking a microglia progenitor cell in the adult brain." Neuron **82**(2): 380-
479 397.

480 Gay, F. W., T. J. Drye, G. W. Dick and M. M. Esiri (1997). "The application of multifactorial cluster analysis in
481 the staging of plaques in early multiple sclerosis. Identification and characterization of the primary
482 demyelinating lesion." Brain **120** (Pt 8): 1461-1483.

483 Gehrman, J., Y. Matsumoto and G. W. Kreutzberg (1995). "Microglia: intrinsic immune effector cell of the
484 brain." Brain Res Brain Res Rev **20**(3): 269-287.

485 Hirota, H., H. Kiyama, T. Kishimoto and T. Taga (1996). "Accelerated Nerve Regeneration in Mice by
486 upregulated expression of interleukin (IL) 6 and IL-6 receptor after trauma." J Exp Med **183**(6): 2627-2634.

487 Hollensworth, S. B., C. Shen, J. E. Sim, D. R. Spitz, G. L. Wilson and S. P. LeDoux (2000). "Glial cell type-
488 specific responses to menadione-induced oxidative stress." Free Radic Biol Med **28**(8): 1161-1174.

489 Holmberg, K. H. and P. H. Patterson (2006). "Leukemia inhibitory factor is a key regulator of astrocytic,
490 microglial and neuronal responses in a low-dose pilocarpine injury model." Brain Res **1075**(1): 26-35.

491 Jiang, J., W. Wen and P. S. Sachdev (2016). "Macrophage inhibitory cytokine-1/growth differentiation factor 15
492 as a marker of cognitive ageing and dementia." Curr Opin Psychiatry **29**(2): 181-186.

493 Kempf, T., M. Eden, J. Strelau, M. Naguib, C. Willenbockel, J. Tongers, J. Heineke, D. Kotlarz, J. Xu, J. D.
494 Molkenstin, H. W. Niessen, H. Drexler and K. C. Wollert (2006). "The transforming growth factor-beta
495 superfamily member growth-differentiation factor-15 protects the heart from ischemia/reperfusion injury." Circ
496 Res **98**(3): 351-360.

497 Kempuraj, D., R. Thangavel, P. A. Natteru, G. P. Selvakumar, D. Saeed, H. Zahoor, S. Zaheer, S. S. Iyer and A.
498 Zaheer (2016). "Neuroinflammation Induces Neurodegeneration." J Neurol Neurosurg Spine **1**(1).

499 Krauspe, B. M., W. Dreher, C. Beyer, W. Baumgartner, B. Denecke, K. Janssen, C. D. Langhans, T. Clarner and
500 M. Kipp (2015). "Short-term cuprizone feeding verifies N-acetylaspartate quantification as a marker of
501 neurodegeneration." J Mol Neurosci **55**(3): 733-748.

502 Kummer, J. A., R. Broekhuizen, H. Everett, L. Agostini, L. Kuijk, F. Martinon, R. van Bruggen and J. Tschopp
503 (2007). "Inflammasome components NALP 1 and 3 show distinct but separate expression profiles in human
504 tissues suggesting a site-specific role in the inflammatory response." J Histochem Cytochem **55**(5): 443-452.

505 Linnane, A. W., S. Marzuki, T. Ozawa and M. Tanaka (1989). "Mitochondrial DNA mutations as an important
506 contributor to ageing and degenerative diseases." Lancet **1**(8639): 642-645.

507 Mahad, D., H. Lassmann and D. Turnbull (2008). "Review: Mitochondria and disease progression in multiple
508 sclerosis." Neuropathol Appl Neurobiol **34**(6): 577-589.

509 Maiti, A. K., S. Sharba, N. Navabi, H. Forsman, H. R. Fernandez and S. K. Lindén (2015). "IL-4 Protects the
510 Mitochondria Against TNF α and IFN γ Induced Insult During Clearance of Infection with *Citrobacter rodentium*
511 and *Escherichia coli*." Scientific Reports **5**: 15434.

512 Mao, P. and P. H. Reddy (2010). "Is multiple sclerosis a mitochondrial disease?" Biochimica et biophysica acta
513 **1802**(1): 66-79.

514 Marik, C., P. A. Felts, J. Bauer, H. Lassmann and K. J. Smith (2007). "Lesion genesis in a subset of patients with
515 multiple sclerosis: a role for innate immunity?" Brain **130**(Pt 11): 2800-2815.

516 Matsumoto, J., S. Dohgu, F. Takata, T. Machida, F. F. Bolukbasi Hatip, I. Hatip-Al-Khatib, A. Yamauchi and Y.
517 Kataoka (2018). "TNF-alpha-sensitive brain pericytes activate microglia by releasing IL-6 through cooperation
518 between IkappaB-NFkappaB and JAK-STAT3 pathways." Brain Res **1692**: 34-44.

519 Merabova, N., R. Kaminski, B. Krynska, S. Amini, K. Khalili and A. Darbinyan (2012). "JCV agnoprotein-
520 induced reduction in CXCL5/LIX secretion by oligodendrocytes is associated with activation of apoptotic
521 signaling in neurons." J Cell Physiol **227**(8): 3119-3127.

522 Mochida, S., T. Yoshimoto, S. Mimura, M. Inao, A. Matsui, A. Ohno, H. Koh, E. Saitoh, S. Nagoshi and K.
523 Fujiwara (2004). "Transgenic mice expressing osteopontin in hepatocytes as a model of autoimmune hepatitis."
524 Biochem Biophys Res Commun **317**(1): 114-120.

525 Moyon, S., A. L. Dubessy, M. S. Aigrot, M. Trotter, J. K. Huang, L. Dauphinot, M. C. Potier, C. Kerninon, S.
526 Melik Parsadaniantz, R. J. Franklin and C. Lubetzki (2015). "Demyelination causes adult CNS progenitors to
527 revert to an immature state and express immune cues that support their migration." J Neurosci **35**(1): 4-20.

528 Okamura, R. M., J. Lebkowski, M. Au, C. A. Priest, J. Denham and A. S. Majumdar (2007). "Immunological
529 properties of human embryonic stem cell-derived oligodendrocyte progenitor cells." J Neuroimmunol **192**(1-2):
530 134-144.

531 Perry, V. H., P. B. Andersson and S. Gordon (1993). "Macrophages and inflammation in the central nervous
532 system." Trends Neurosci **16**(7): 268-273.

533 Petkovic, F., I. L. Campbell, B. Gonzalez and B. Castellano (2017). "Reduced cuprizone-induced cerebellar
534 demyelination in mice with astrocyte-targeted production of IL-6 is associated with chronically activated, but
535 less responsive microglia." J Neuroimmunol **310**: 97-102.

536 Puthalakath, H., L. A. O'Reilly, P. Gunn, L. Lee, P. N. Kelly, N. D. Huntington, P. D. Hughes, E. M. Michalak,
537 J. McKimm-Breschkin, N. Motoyama, T. Gotoh, S. Akira, P. Bouillet and A. Strasser (2007). "ER stress triggers
538 apoptosis by activating BH3-only protein Bim." Cell **129**(7): 1337-1349.

539 Ramesh, G., S. Benge, B. Pahar and M. T. Philipp (2012). "A possible role for inflammation in mediating
540 apoptosis of oligodendrocytes as induced by the Lyme disease spirochete *Borrelia burgdorferi*." J
541 Neuroinflammation **9**: 72.

542 Richter-Landsberg, C. and M. Heinrich (1996). "OLN-93: a new permanent oligodendroglia cell line derived
543 from primary rat brain glial cultures." J Neurosci Res **45**(2): 161-173.

544 Ridker, P. M., N. Rifai, M. J. Stampfer and C. H. Hennekens (2000). "Plasma concentration of interleukin-6 and
545 the risk of future myocardial infarction among apparently healthy men." Circulation **101**(15): 1767-1772.

546 Ruther, B. J., M. Scheld, D. Drey Mueller, T. Clarner, E. Kress, L. O. Brandenburg, T. Swartenbroekx, C.
547 Hoornaert, P. Ponsaerts, P. Fallier-Becker, C. Beyer, S. O. Rohr, C. Schmitz, U. Chrzanowski, T. Hochstrasser,
548 S. Nyamoya and M. Kipp (2017). "Combination of cuprizone and experimental autoimmune encephalomyelitis
549 to study inflammatory brain lesion formation and progression." Glia **65**(12): 1900-1913.

550 Rutkowski, D. T., S. M. Arnold, C. N. Miller, J. Wu, J. Li, K. M. Gunnison, K. Mori, A. A. Sadighi Akha, D.
551 Raden and R. J. Kaufman (2006). "Adaptation to ER stress is mediated by differential stabilities of pro-survival
552 and pro-apoptotic mRNAs and proteins." PLoS Biol **4**(11): e374.

553 Scheld, M., B. J. Ruther, R. Grosse-Veldmann, K. Ohl, K. Tenbrock, D. Drey Muller, P. Fallier-Becker, A.
554 Zendedel, C. Beyer, T. Clarner and M. Kipp (2016). "Neurodegeneration Triggers Peripheral Immune Cell
555 Recruitment into the Forebrain." J Neurosci **36**(4): 1410-1415.

556 Schlittenhardt, D., W. Schmiedt, G. A. Bonaterra, J. Metz and R. Kinscherf (2005). "Colocalization of oxidized
557 low-density lipoprotein, caspase-3, cyclooxygenase-2, and macrophage migration inhibitory factor in
558 arteriosclerotic human carotid arteries." Cell Tissue Res **322**(3): 425-435.

559 Schonrock, L. M., G. Gawlowski and W. Bruck (2000). "Interleukin-6 expression in human multiple sclerosis
560 lesions." Neurosci Lett **294**(1): 45-48.

561 Seino, Y., U. Ikeda, M. Ikeda, K. Yamamoto, Y. Misawa, T. Hasegawa, S. Kano and K. Shimada (1994).
562 "Interleukin 6 gene transcripts are expressed in human atherosclerotic lesions." Cytokine **6**(1): 87-91.

563 Selvaraju, R., L. Bernasconi, C. Losberger, P. Graber, L. Kadi, V. Avellana-Adalid, N. Picard-Riera, A. Baron
564 Van Evercooren, R. Cirillo, M. Kosco-Vilbois, G. Feger, R. Papoian and U. Boschert (2004). "Osteopontin is
565 upregulated during in vivo demyelination and remyelination and enhances myelin formation in vitro." Mol Cell
566 Neurosci **25**(4): 707-721.

567 Škuljec, J., H. Sun, R. Pul, K. Bénardais, D. Ragancokova, D. Moharreggh-Khiabani, A. Kotsiari, C. Trebst and
568 M. Stangel (2011). "CCL5 induces a pro-inflammatory profile in microglia in vitro." Cellular Immunology
569 **270**(2): 164-171.

570 Su, K., D. Bourdette and M. Forte (2013). "Mitochondrial dysfunction and neurodegeneration in multiple
571 sclerosis." Front Physiol **4**: 169.

572 Sugiura, S., R. Lahav, J. Han, S. Y. Kou, L. R. Banner, F. de Pablo and P. H. Patterson (2000). "Leukaemia
573 inhibitory factor is required for normal inflammatory responses to injury in the peripheral and central nervous
574 systems in vivo and is chemotactic for macrophages in vitro." Eur J Neurosci **12**(2): 457-466.

575 Swardfager, W., K. Lanctot, L. Rothenburg, A. Wong, J. Cappell and N. Herrmann (2010). "A meta-analysis of
576 cytokines in Alzheimer's disease." Biol Psychiatry **68**(10): 930-941.

577 Teske, N., A. Liessem, F. Fischbach, T. Clarner, C. Beyer, C. Wruck, A. Fragoulis, S. C. Tauber, M. Victor and
578 M. Kipp (2018). "Chemical hypoxia-induced integrated stress response activation in oligodendrocytes is
579 mediated by the transcription factor nuclear factor (erythroid-derived 2)-like 2 (NRF2)." J Neurochem **144**(3):
580 285-301.

581 Tezuka, T., M. Tamura, M. A. Kondo, M. Sakaue, K. Okada, K. Takemoto, A. Fukunari, K. Miwa, H. Ohzeki, S.
582 Kano, H. Yasumatsu, A. Sawa and Y. Kajii (2013). "Cuprizone short-term exposure: astrocytic IL-6 activation
583 and behavioral changes relevant to psychosis." Neurobiol Dis **59**: 63-68.

584 Tsui, K. H., Y. L. Chang, T. H. Feng, L. C. Chung, T. Y. Lee, P. L. Chang and H. H. Juang (2012). "Growth
585 differentiation factor-15 upregulates interleukin-6 to promote tumorigenesis of prostate carcinoma PC-3 cells." J
586 Mol Endocrinol **49**(2): 153-163.

587 Tzartos, J. S., M. A. Friese, M. J. Craner, J. Palace, J. Newcombe, M. M. Esiri and L. Fugger (2008).
588 "Interleukin-17 production in central nervous system-infiltrating T cells and glial cells is associated with active
589 disease in multiple sclerosis." Am J Pathol **172**(1): 146-155.

590 van der Valk, P. and S. Amor (2009). "Preactive lesions in multiple sclerosis." Curr Opin Neurol **22**(3): 207-213.

591 Wang, C. H., S. B. Wu, Y. T. Wu and Y. H. Wei (2013). "Oxidative stress response elicited by mitochondrial
592 dysfunction: implication in the pathophysiology of aging." Exp Biol Med (Maywood) **238**(5): 450-460.

593 Wruck, C. J., K. Streetz, G. Pavic, M. E. Gotz, M. Tohidnezhad, L. O. Brandenburg, D. Varoga, O. Eickelberg,
594 T. Herdegen, C. Trautwein, K. Cha, Y. W. Kan and T. Pufe (2011). "Nrf2 induces interleukin-6 (IL-6)
595 expression via an antioxidant response element within the IL-6 promoter." J Biol Chem **286**(6): 4493-4499.

596 Wuerfel, J., J. Bellmann-Strobl, P. Brunecker, O. Aktas, H. McFarland, A. Villringer and F. Zipp (2004).
597 "Changes in cerebral perfusion precede plaque formation in multiple sclerosis: a longitudinal perfusion MRI
598 study." Brain **127**(Pt 1): 111-119.

- 599 Yang, P., H. Wen, S. Ou, J. Cui and D. Fan (2012). "IL-6 promotes regeneration and functional recovery after
600 cortical spinal tract injury by reactivating intrinsic growth program of neurons and enhancing synapse
601 formation." Exp Neurol **236**(1): 19-27.
- 602 Yang, R., D. Lirussi, T. M. Thornton, D. M. Jelley-Gibbs, S. A. Diehl, L. K. Case, M. Madesh, D. J. Taatjes, C.
603 Teuscher, L. Haynes and M. Rincon (2015). "Mitochondrial Ca(2)(+) and membrane potential, an alternative
604 pathway for Interleukin 6 to regulate CD4 cell effector function." Elife **4**.
- 605 Yumoto, K., M. Ishijima, S. R. Rittling, K. Tsuji, Y. Tsuchiya, S. Kon, A. Nifuji, T. Uede, D. T. Denhardt and
606 M. Noda (2002). "Osteopontin deficiency protects joints against destruction in anti-type II collagen antibody-
607 induced arthritis in mice." Proc Natl Acad Sci U S A **99**(7): 4556-4561.
- 608 Zeis, T., A. Probst, A. J. Steck, C. Stadelmann, W. Bruck and N. Schaeren-Wiemers (2009). "Molecular changes
609 in white matter adjacent to an active demyelinating lesion in early multiple sclerosis." Brain Pathol **19**(3): 459-
610 466.
- 611 Zhang, X., S. Tachibana, H. Wang, M. Hisada, G. M. Williams, B. Gao and Z. Sun (2010). "Interleukin-6 is an
612 important mediator for mitochondrial DNA repair after alcoholic liver injury in mice." Hepatology **52**(6): 2137-
613 2147.